

${}^7\text{Li} + {}^{12}\text{C}$: Excitation of projectile and target states and single-nucleon stripping

J. Cook

Department of Physics, University of Petroleum and Minerals, Dhahran 31261, Saudi Arabia

M. N. Stephens and K. W. Kemper

Department of Physics, The Florida State University, Tallahassee, Florida 32306

A. K. Abdallah

Department of Physics, University of Petroleum and Minerals, Dhahran 31261, Saudi Arabia

(Received 29 October 1985)

Detailed cross sections out to 170° c.m. for elastic scattering and the excitation of states in ${}^7\text{Li}$ and in ${}^{12}\text{C}$ have been determined by bombarding ${}^{12}\text{C}$ targets with 34 MeV ${}^7\text{Li}$ beams and ${}^7\text{Li}$ targets with ${}^{12}\text{C}$ beams at the same c.m. energy. The present results show that the direct breakup total cross section for ${}^7\text{Li}$ is about 25 times larger than the sequential total cross section to the $\frac{7}{2}^-$ 4.63 MeV state of ${}^7\text{Li}$. In addition, single neutron and proton stripping angular distributions have been measured. The distorted-wave Born approximation is unsatisfactory for the excitation of the $\frac{1}{2}^-$ 0.48 MeV state of ${}^7\text{Li}$, the 2^+ 4.44 MeV state of ${}^{12}\text{C}$, and the mutual excitation of these two states. Coupled channels calculations, using the rotation-vibration model, describe the excitation of states in ${}^{12}\text{C}$ well and find $K=3$ for the 3^- 9.64 MeV state. Poor fits are obtained to the projectile and mutual excitation data with coupled channels calculations. Finite range distorted-wave Born approximation calculations of single-nucleon stripping are in good agreement with the data. Extracted deformation lengths and spectroscopic factors are consistent with those from other studies.

I. INTRODUCTION

The interaction between two lighter heavy ions gives rise to a rich and complex series of reactions. At energies of 5–10 MeV per nucleon peripheral reactions are dominated by elastic, inelastic, and single-nucleon transfer reactions. When one of the interaction partners is loosely bound, like ${}^7\text{Li}$ ($E_B=2.47$ MeV), breakup, either direct or sequential, can become an additional important degree of freedom at relatively low bombarding energies. The lower level density present in the light systems usually means that the state being populated can be isolated so that less ambiguity is present in knowing the exact reaction taking place. In the present work, a detailed study of the system ${}^7\text{Li} + {}^{12}\text{C}$ has been undertaken at a laboratory energy of 34 MeV. Elastic and inelastic angular distributions out to 170° are presented. In addition, cross sections for the unbound $\frac{7}{2}^-$, 4.63 MeV state in ${}^7\text{Li}$ and the continuum excitation of ${}^7\text{Li}$ are reported. Single proton and neutron transfer angular distributions are also reported.

The present data are analyzed in terms of the distorted-wave Born approximation (DWBA) and the coupled channels (CC) methods. A rotational model for ${}^7\text{Li}$ and a rotation-vibration model (RVM) for ${}^{12}\text{C}$ are used for treatment of the inelastic excitations. Deformed Woods-Saxon potentials are employed, and the parameters are adjusted in CC calculations to optimize the fits to the data. Calculations are made for projectile and target excitation separately, and also for the two together, including mutual excitation. Finite-range DWBA calculations are made for the (${}^7\text{Li}, {}^6\text{Li}$) and (${}^7\text{Li}, {}^6\text{He}$) reaction data. Deformation lengths and spectroscopic factors are determined

and are compared with the results of other studies.

In Sec. II the experimental procedure to measure the data is described, and in Sec. III the inelastic scattering data are analyzed. The single-nucleon transfer calculations are described in Sec. IV. The results are discussed in Sec. V and the conclusions presented there.

II. EXPERIMENTAL PROCEDURE

In the present work, two separate sets of measurements were made. The first series of measurements was to determine the angular distributions and cross sections for ${}^7\text{Li} + {}^{12}\text{C}$ elastic and inelastic scattering and the single neutron and proton transfer reactions for forward angles ($<100^\circ$ laboratory) and were carried out by bombarding a ${}^{12}\text{C}$ target with a ${}^7\text{Li}$ beam and detecting the scattered ${}^7\text{Li}$. The second series of measurements determined the elastic and inelastic cross sections for angles between 100° laboratory and 168° laboratory as well as the inelastic cross sections to the unbound states of ${}^7\text{Li}$ by scattering a ${}^{12}\text{C}$ beam from a ${}^7\text{Li}$ target and detecting both the scattered ${}^{12}\text{C}$ particles and the recoil ${}^7\text{Li}$ particles.

In this work three beams (p , ${}^7\text{Li}$, and ${}^{12}\text{C}$) were produced and accelerated with the Florida State University super FN tandem accelerator facility. The ${}^7\text{Li}$ beam energy was 34 MeV and that for ${}^{12}\text{C}$ was about 58.4 MeV, with its exact energy chosen so that both beams had the same c.m. energy at the center of their respective targets. The ${}^{12}\text{C}$ targets were self-supporting natural carbon films (98.9% ${}^{12}\text{C}$) with thicknesses of about $100 \mu\text{g}/\text{cm}^2$. Because Li turns to LiOH readily upon exposure to humid air, natural Li (92.4% ${}^7\text{Li}$) vapor was deposited on Form-

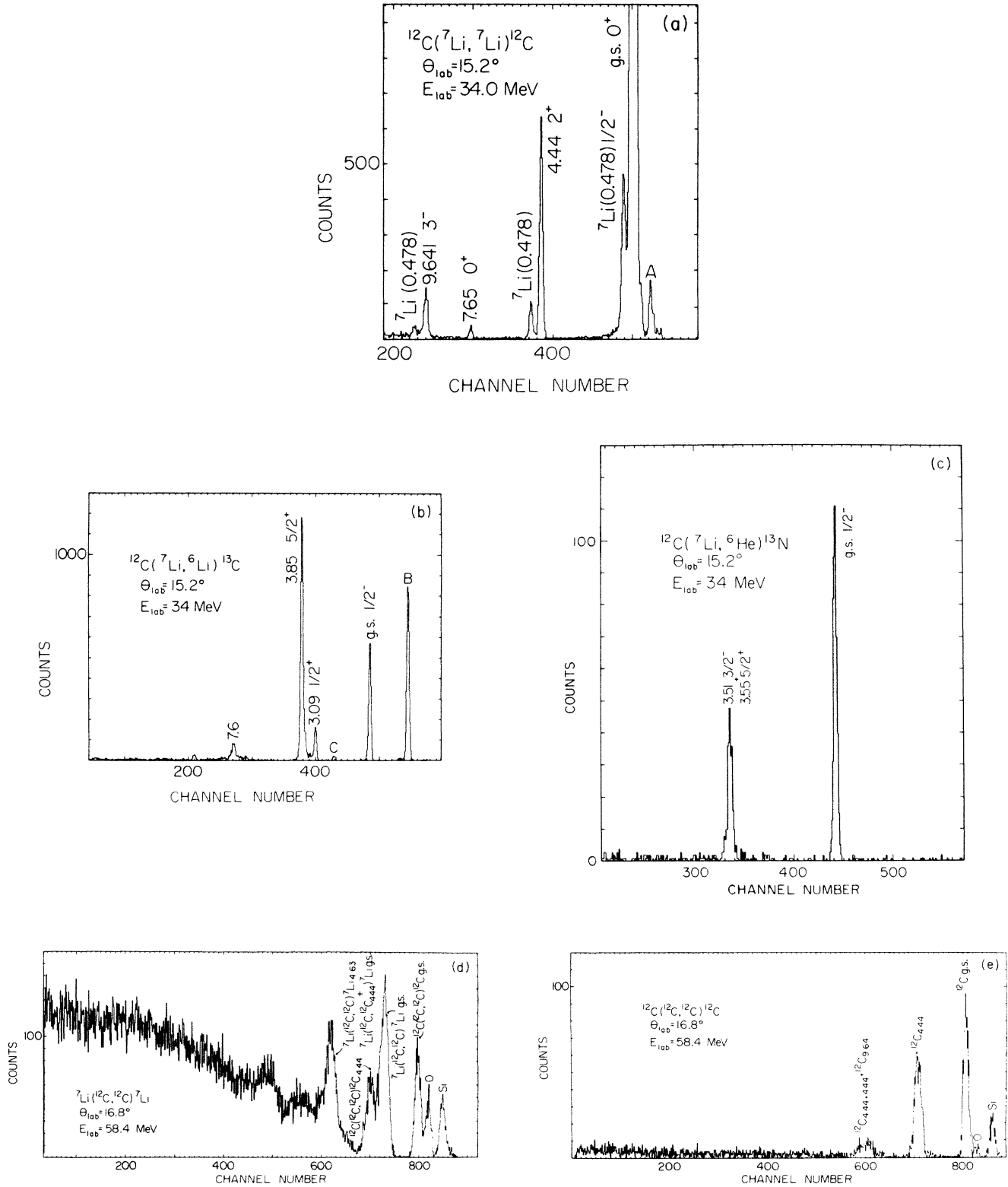


FIG. 1. (a) Elastic and inelastic scattering spectrum for $^7\text{Li} + ^{12}\text{C}$. The elastic peak has a maximum yield per channel of 10^4 counts at this angle. The peak labeled A arises from oxygen contamination on the target. (b) Sample spectrum for the $^{12}\text{C}(^7\text{Li}, ^6\text{Li})^{13}\text{C}$ reaction. The peaks labeled B and C arise from spillover of the intense elastic (B) and 4.44 MeV inelastic (C) ^7Li events into the ^6Li group. (c) Sample spectrum for the $^{12}\text{C}(^7\text{Li}, ^6\text{He})^{13}\text{N}$ reaction. (d) Sample ^{12}C spectrum obtained when a ^7Li target is bombarded by a ^{12}C beam. The peaks labeled Si and O arise from contamination of the ^7Li sample used to make the target, and those labeled ^{12}C come from the target backing. (e) Sample ^{12}C spectrum obtained from a ^{12}C target. The height of the elastic peak has been normalized to that in (d), so that the difference in the continuum yield between the ^7Li target and the ^{12}C target is readily apparent.

var backings in a target barrel which could be transferred into the scattering chamber under vacuum. The ${}^7\text{Li}$ targets had thicknesses between 30 and 50 $\mu\text{g}/\text{cm}^2$.

Silicon surface barrier $\Delta E \times E$ counter telescopes were used throughout the measurements so that particle identification of the reaction products could be carried out. A stationary monitor detector allowed the beam integration and target condition to be continuously checked.

To determine the absolute cross sections, a knowledge of the product of the target thickness times the solid angle ($Nd\Omega$) is needed. To determine $Nd\Omega$ for the ${}^{12}\text{C}$ target, 20 MeV ${}^{16}\text{O}$ elastic scattering was measured in the angular range from 14° – 20° laboratory, and found to follow Rutherford scattering. This measurement along with the beam charge state found from other measurements allowed $Nd\Omega$ to be determined. Another check on this value was to measure proton elastic scattering from the ${}^{12}\text{C}$ target and to use the previously reported cross sections of Bernard *et al.*¹ to determine $Nd\Omega$. The two results agreed to $\pm 8\%$ so that the absolute uncertainty in the present measurements is $\pm 9\%$ when the uncertainties in beam integration and angle settings are included.

The ${}^7\text{Li}$ target thickness ($Nd\Omega$) was determined by overlapping the recoil measurements with the ${}^7\text{Li}$ scattering data. To make certain that the factor of 10 smaller large angle cross sections observed for ${}^7\text{Li}$ scattering when compared with ${}^6\text{Li} + {}^{12}\text{C}$ scattering were correct, the ${}^7\text{Li}$ target thickness ($Nd\Omega$) was also determined by scattering protons from the ${}^7\text{Li}$ target and assuming the cross sections previously determined by Bingham *et al.*² The two values obtained for $Nd\Omega$ agreed to within $\pm 7\%$.

An important part of the present work was to determine the cross section for populating the 4.63 MeV state

in ${}^7\text{Li}$. Strong excitation of this state would signal a need to include this state in attempts to describe the ${}^7\text{Li} + {}^{12}\text{C}$ interaction process. The 4.63 MeV state is unbound to decay into $\alpha + t$ so that it is not present in the ${}^7\text{Li}$ spectrum. To determine this cross section, spectra of the ${}^{12}\text{C}$ projectiles scattered by ${}^7\text{Li}$, ${}^{12}\text{C}$, and SiO_2 targets were taken at 14 angles. Occurring at about the same location in the spectrum as the 4.63 MeV peak, is the peak corresponding to ${}^7\text{Li}(\text{g.s.}) + {}^{12}\text{C}(4.44 \text{ MeV})$. The combined yield was found for the peak. The ${}^{12}\text{C}(4.44 \text{ MeV})$ cross section that had been previously determined from the forward scattering measurements allowed the ${}^{12}\text{C}(4.44 \text{ MeV})$ yield to be subtracted so that the ${}^7\text{Li}$, 4.63 MeV cross section could be determined. The total cross section for excitation of this state was found to be 32 mb. In addition, the continuum yield was added at each angle and yielded a cross section of $900 \pm 100 \text{ mb}$ for the excitation region in ${}^7\text{Li}$ between 6 and 24 MeV after subtraction of contributions from the ${}^{12}\text{C}$, Si, and O contaminants on the Li target.

Typical spectra for the reactions reported in this work are shown in Fig. 1. By comparing the ${}^{12}\text{C} + {}^{12}\text{C}$ and ${}^{12}\text{C} + {}^7\text{Li}$ spectra it can be seen that the continuum yield for ${}^{12}\text{C} + {}^7\text{Li}$ is associated with the ${}^7\text{Li}$ target and not instrumental. Also, the population of the $\frac{1}{2}^+$ state in ${}^{13}\text{C}$ and its absence in ${}^{13}\text{N}$ is striking evidence of the important role played by angular momentum mismatch in these reactions.

III. INELASTIC SCATTERING DATA

A. DWBA analysis

The distorted-wave Born approximation calculations were performed with an extended version of the computer

TABLE I. Potential parameters and deformation lengths for inelastic scattering. [The same geometry was used for all calculations: $r_R = 0.63 \text{ fm}$, $a_R = 0.73 \text{ fm}$, $r_I = 1.38 \text{ fm}$, $a_I = 0.85 \text{ fm}$, $r_c = 1.25 \text{ fm}$ with $R_x = r_x(7^{1/3} + 12^{1/3})$].

Description	Type	V (MeV)	W (MeV)	$\delta_2({}^7\text{Li})$ (fm)	$\delta_2({}^{12}\text{C})$ (fm)	$\delta_{3K}({}^{12}\text{C})$ (fm)
	DWBA	159	7.2	2.00	-1.40	1.11 ^a 0.82 ^b
${}^7\text{Li } \frac{3}{2}^- - \frac{1}{2}^-$	CC	175	7.8	2.00		
${}^7\text{Li } \frac{3}{2}^- - \frac{1}{2}^- - \frac{7}{2}^-$	CC	159	7.0	2.00		
${}^{12}\text{C } 0^+ - 2^+$	CC	147	6.6		-1.40	
${}^{12}\text{C } 0^+ - 2^+ - 3^-^a$	CC	145	6.8		-1.40	1.25
${}^{12}\text{C } 0^+ - 2^+ - 3^-^b$	CC	143	8.2		-1.40	0.88
${}^7\text{Li } \frac{3}{2}^- - \frac{1}{2}^-$	CC	143	8.2	1.35	-1.05	0.88
${}^{12}\text{C } 0^+ - 2^+ - 3^-^a$						
${}^7\text{Li } \frac{1}{2}^- + {}^{12}\text{C } 2^+$						

^a $K=0$ for 3^- state of ${}^{12}\text{C}$.

^b $K=3$ for 3^- state of ${}^{12}\text{C}$.

code CHUCK3.³ The distorted waves were generated with the Woods-Saxon optical potentials which had previously⁴ been found to fit the elastic scattering data of ${}^7\text{Li} + {}^{12}\text{C}$ at 34 MeV. Deformed Woods-Saxon form factors were used and Coulomb excitation was included. The same deformation lengths were used for the real and imaginary potentials and for the Coulomb excitation contributions. The three potentials VII, VIII, and IX in Table I of Ref. 4 were used, giving very similar DWBA predictions for the inelastic states. This is not surprising since these potentials yield almost identical fits to the elastic scattering. Figure 2 shows the fit to the elastic data using potential VII and the inelastic predictions in that figure are all based upon this potential. The deformation parameters obtained are listed in Table I.

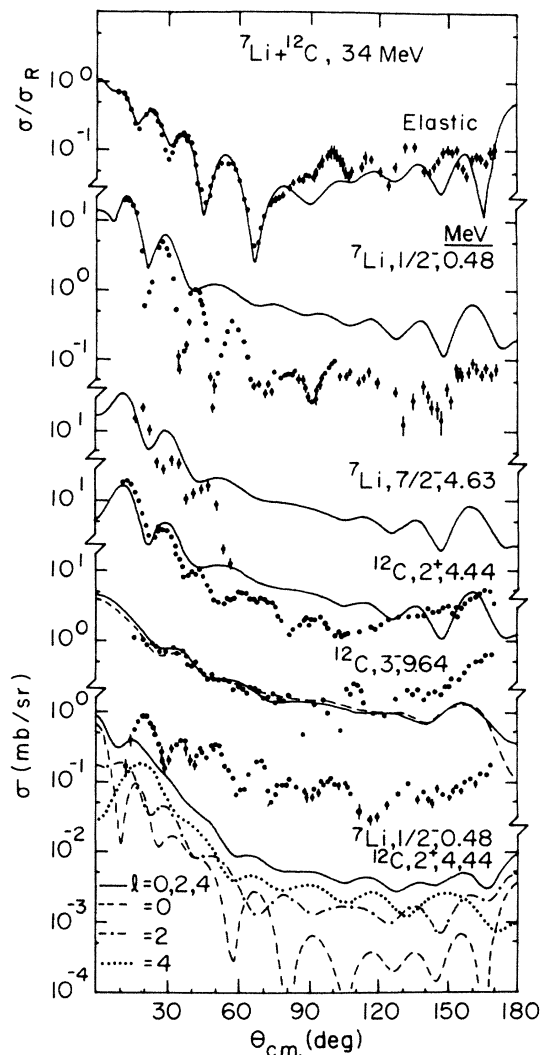


FIG. 2. Optical model fit to ${}^7\text{Li} + {}^{12}\text{C}$ elastic scattering data at 34 MeV and DWBA predictions for inelastic scattering to states in ${}^7\text{Li}$, states in ${}^{12}\text{C}$, and the mutual excitation of ${}^7\text{Li}$ and ${}^{12}\text{C}$. A rotational model was used for ${}^7\text{Li}$ and the rotation-vibration model for ${}^{12}\text{C}$. Potential set VII from Ref. 4 was used to generate the distorted waves. The deformation lengths are listed in Table I. The two lines for the 3^- state in ${}^{12}\text{C}$ are calculations assuming it to be $K=0$ (dashed line) and $K=3$ (full line).

For the projectile excitation to the $\frac{1}{2}^-$ 0.478 MeV state of ${}^7\text{Li}$ a deformation length of 2.0 fm is required to obtain the magnitude of the first maximum at about 13° correctly. Thereafter the description of the data is poor, being unable to account for the phasing of the next oscillations and the magnitude of the large angle data. This is a common problem (e.g., Refs. 5–7) for the excitation of this state in ${}^7\text{Li}$, one that is usually solved by resorting to coupled channels calculations. The same deformation length of 2.0 fm provides approximately the correct magnitude for excitation of the $\frac{7}{2}^-$ 4.63 MeV state in ${}^7\text{Li}$, but the prediction can hardly be said to be a faithful representation of the data. In a rigid rotor model these two quadrupole deformation lengths should be equal, and thus these results would indicate that this model has some validity for ${}^7\text{Li}$.

The 2^+ 4.44 MeV state of ${}^{12}\text{C}$ was treated as a member of the ground-state rotational band of ${}^{12}\text{C}$. A deformation length of 1.40 fm in magnitude provides the best compromise for fitting the first two maxima in the angular distribution. The slope of the prediction is not correct, the calculated cross sections being too small for the first oscillation, and too large subsequently. The calculations are also incorrect in phase due to the absence of the reorientation term for the 2^+ state in the DWBA. These are problems that may usually be circumvented in coupled channels calculations. The 3^- 9.64 MeV state of ${}^{12}\text{C}$ was treated in the rotation-vibration model as an octupole vibration based upon the ground state. The state was considered as either $K=0$ or $K=3$ which yielded octupole deformation lengths of 1.11 and 0.82 fm, respectively, with very similar angular distributions which describe the data well for $\theta < 80^\circ$. For larger angles the data show some oscillatory structure and a rise in magnitude whereas the calculations do not.

Finally the mutual excitation of ${}^7\text{Li}$ to its $\frac{1}{2}^-$ 0.478 MeV state and ${}^{12}\text{C}$ to its 2^+ 4.44 MeV state was considered. In the DWBA this involves the simultaneous excitation of both nuclei. Since the excitation of each nucleus separately is of quadrupole type, relative angular momenta transfer of $l=0, 2,$ and 4 are possible for the mutual excitation. Figure 2 shows each contribution separately and also their sum. The calculations were made with deformation lengths of 2.0 fm for ${}^7\text{Li}$ and 1.4 fm for ${}^{12}\text{C}$, the values found for excitation of the projectile or target alone. The figure shows that the DWBA cannot explain this data. The experimental data clearly exhibit oscillations for $\theta < 80^\circ$, while the calculations decrease steadily for $\theta < 60^\circ$, and then flatten off at about $\frac{1}{10}$ of the experimental cross section. Even the magnitude and shape of the very forward angles are not correct. As has been found in previous^{5,8} calculations the $l=4$ contribution is the most important, then $l=2$ and lastly $l=0$.

In summary, the DWBA calculations fail to describe the excitation of ${}^7\text{Li}$ and ${}^{12}\text{C}$ to their first $\frac{1}{2}^-$ and 2^+ states, respectively. This is to be expected since both states are strongly excited and therefore coupled channels calculations should be employed. Previous DWBA studies^{5–7} of ${}^7\text{Li} + {}^{12}\text{C}$ inelastic scattering have always found the $\frac{1}{2}^-$ state of ${}^7\text{Li}$ to be poorly described in phase, but reasonable fits to the 2^+ state of ${}^{12}\text{C}$ were obtained. The

3^- state of ${}^{12}\text{C}$ is weakly coupled to the ground state and thus the DWBA works well, but is unable to distinguish between $K=0$ and $K=3$. The mutual excitation data and DWBA calculations have little resemblance to each other.

B. Coupled channels analysis

The inelastic data were also analyzed by means of coupled channels calculations carried out with an extended version of the computer code CHUCK3.³ At first, excitations in the projectile and target were treated separately, using a rigid rotor model for ${}^7\text{Li}$ and the rotation-vibration model for ${}^{12}\text{C}$. Later, projectile and target excitations were included in the same calculation simultaneously, together with mutual excitation. All calculations were made starting from potential VII of Table I in Ref. 4.

The computer time consumed was too excessive to enable a full study to be made with the other two potentials that fitted the elastic scattering data, but some trial calculations showed that the results did not differ significantly. As a guide to the amount of computer time involved, on the Amdahl 5850 computer at the University of Petroleum and Minerals, the projectile excitation calculations took about 40 sec, and those for target excitation 4 sec for 0^+-2^+ coupling and 30 sec for $0^+-2^+-3^-$ coupling. Calculations for projectile and target excitation together took about 20 min excluding mutual excitation, and about 30 min including it.

1. Projectile excitation

Calculations were first made coupling the ground state of ${}^7\text{Li}$ and its $\frac{1}{2}^-$ 0.478 MeV state together using a rotational model. The ground state reorientation term and Coulomb excitation were included. A deformation length of 2.0 fm gave the correct magnitude to the first two maxima of the inelastic scattering using potential VII. The phasing of the elastic scattering for $\theta=40^\circ-90^\circ$ was poor and the calculations had little resemblance to the inelastic scattering in the same angular range. The potential parameters were now varied to improve the fits resulting in the dashed line shown in Fig. 3 and the parameters given in Table I. It was found necessary to increase the depth of the real potential from 159 to 175 MeV, and to change the depth of the imaginary potential from 7.2 to 7.8 MeV. Changes in the other parameters did not improve the fits. The elastic scattering was then described better, although it was incorrect in phase at the minimum at 67° by about 5° . The fit to the inelastic scattering was still very poor, being unable to describe the diffraction structure for $\theta < 65^\circ$. Extensive parameter searching was unable to improve these fits.

The $\frac{7}{2}^-$ 4.63 MeV state of ${}^7\text{Li}$ was now coupled into the calculations. The reorientation term for the $\frac{7}{2}^-$ state and $l=4$ transitions were found to have a negligible effect. Again extensive parameter searches were made with a deformation length of 2.0 fm. These resulted in the full lines of Fig. 3 and the potential of Table I. The elastic scattering was now described even worse than before, being unable to fit the oscillations for $\theta=30^\circ-70^\circ$. The fit

to the inelastic scattering to the $\frac{1}{2}^-$ state was much the same as before, and the $\frac{7}{2}^-$ state had the correct magnitude, but even with the small amount of data measured could not be said to be in more than qualitative agreement with it.

It must therefore be concluded that we are unable to describe the inelastic scattering of ${}^7\text{Li} + {}^{12}\text{C}$ at 34 MeV to states in ${}^7\text{Li}$ with a rotational model employing deformed Woods-Saxon potentials in coupled channels calculations. The only other published coupled channels calculations for ${}^7\text{Li} + {}^{12}\text{C}$ are in Ref. 8 for 63 and 79 MeV. Good fits were obtained there to the elastic and projectile excitation data for the $\frac{1}{2}^-$ state. The results reported here are the first for excitation of the $\frac{7}{2}^-$ state.

2. Target excitation

Inelastic scattering to states in ${}^{12}\text{C}$ was considered using the rotation-vibration (RVM) model. Some details of the structure of ${}^{12}\text{C}$ and the form factors in this model have been given in previous papers.^{9,10} The 0^+ ground state and the 2^+ 4.44 MeV states are the first two states of a well-developed rotational band with $K^\pi=0^+$ based upon a permanently deformed ground state. The 3^- 9.64 MeV state is treated as an octupole vibration built on the ground state and can have K^π values from 0^- to 3^- .

Firstly the ground state and 2^+ states were coupled together. A deformation length of -1.40 fm was found to

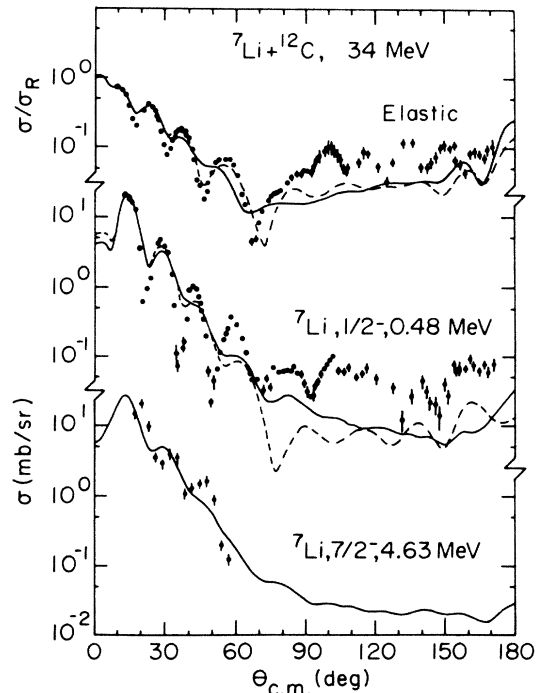


FIG. 3. Comparison of coupled channels calculations with experimental data for excitation of states in ${}^7\text{Li}$ using a rotational model. The dashed lines are the results obtained when just the $\frac{3}{2}^-$ ground state and $\frac{1}{2}^-$ 0.478 MeV state are coupled together, and the full lines show the results when the $\frac{7}{2}^-$ 4.63 MeV state is also included. The potential parameters and deformation lengths are listed in Table I.

produce the correct magnitude to the forward angles of the 2^+ distribution, and in comparison with the DWBA calculations the first and second maxima now had the correct relative magnitudes. The phasing at forward angles improved when a reorientation term for the 2^+ state was included and unambiguously determined the sign of the deformation length to be negative. The best fits were obtained when the real and imaginary potential well depths were changed to 147 MeV and 6.6 MeV, respectively. The fits are shown as the dotted lines in Fig. 4 with the parameters given in Table I. The elastic scattering is well described up to 80° but is too small in magnitude for larger angles. The inelastic scattering is reasonably well fitted up to 50° , but also is too small at larger angles.

The 3^- 9.64 MeV state was now included in the calculations and was treated as either $K^\pi=0^-$ or 3^- . The most important couplings were found to be the $l=3$ direct

term between the 0^+ and 3^- states and then the $l=3$ coupling between the 2^+ and 3^- states. The $l=1$ and 5 couplings between the 2^+ and 3^- states were found to have a negligible effect, similarly for the reorientation term for the 3^- state. The potential depths and the octupole deformation length δ_{3K} were adjusted to produce the best fit to all three states simultaneously. (See Refs. 9 and 10 for a definition of δ_{3K} . The subscript 3 refers to the fact that it is an octupole deformation, and the subscript K denotes the body-fixed component of angular momentum for the band.) It was found that changes in W and δ_{3K} were correlated with each other. The final potential parameters are listed in Table I and the fits are shown as the dashed and full lines in Fig. 4 when the 3^- state is treated as $K^\pi=0^-$ and 3^- , respectively.

The elastic scattering is equally well described in both cases for $\theta < 70^\circ$. At larger angles the calculated angular distribution is just shifted upwards or downwards in magnitude. When the 3^- state is treated as $K=3$ the correct magnitude for the large angle elastic scattering is obtained. The forward angle inelastic scattering for the 2^+ state is very similar in both cases. For $\theta > 70^\circ$ the cross sections become much smaller when the 3^- state is included if it has $K=0$, and a little larger if it has $K=3$. Inelastic scattering to the 3^- state is described correctly in magnitude and slope when it has $K=3$ and $\delta_{3K}=0.88$ fm. The calculations fail to reproduce the oscillations around 90° and the rise in cross section for $\theta > 140^\circ$. It is not possible to describe the 3^- state with $K=0$ when good fits to the elastic scattering and the 2^+ state are simultaneously required.

It is concluded that the RVM can be successfully applied to the excitation of states in ^{12}C via $^7\text{Li} + ^{12}\text{C}$ inelastic scattering at 34 MeV. The 0^+ and 2^+ states are members of the ground state rotational band and the 3^- state is a $K^\pi=3^-$ octupole vibration state. The quadrupole and octupole deformation lengths are $\delta_2 = -1.40$ fm and $\delta_{3K} = 0.88$ fm. No analysis was performed for the data to the 0^+ 7.65 MeV state in ^{12}C because of the uncertain structure of this state. The data are presented in Fig. 4 for completeness.

3. Mutual excitation

Calculations were now made in which excited states of ^7Li and ^{12}C were included in the same calculation simultaneously. It was not possible to perform extensive parameter searches because of the prohibitive amount of computer time involved.

Initially the elastic scattering, the $\frac{1}{2}^-$ state of ^7Li , and the 2^+ and 3^- states of ^{12}C were included in the calculations. Couplings between states in the same nucleus were included, but not between states in different nuclei. The 3^- state of ^{12}C was treated as $K^\pi=3^-$ since this was preferred in the target excitation calculations. The deformation lengths previously found were used, with potential depths $V=143$ MeV and $W=8.2$ MeV. These parameters gave a reasonable description of the target excitation and it was thought preferable to use these rather than the optical model or projectile excitation potential parameters which do not describe the data well in coupled channels

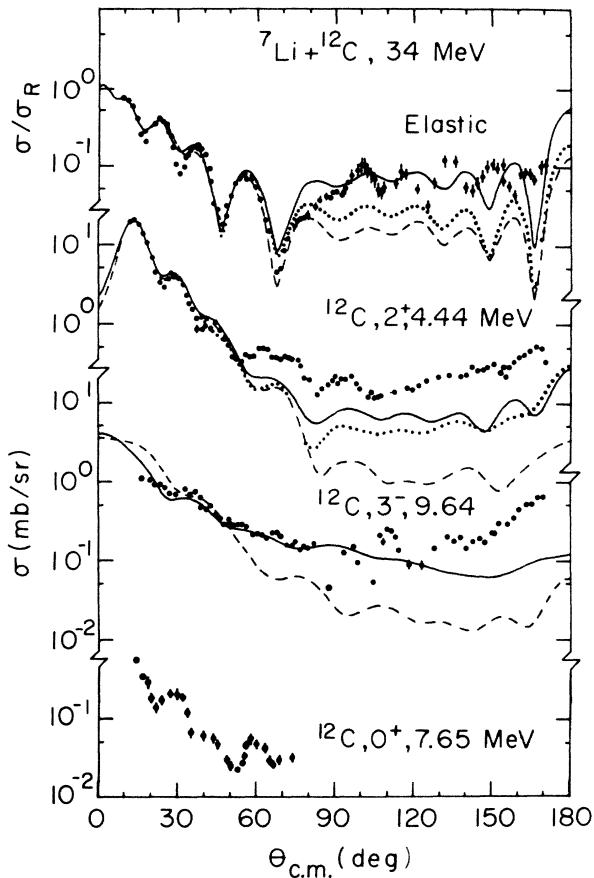


FIG. 4. Experimental data for inelastic scattering to states in ^{12}C compared with coupled channels calculations. The rotation-vibration model was assumed for ^{12}C . Calculations in which only the 0^+ ground state and 2^+ 4.44 MeV state were coupled together are shown as the dotted lines. The dashed and full lines show, respectively, the results of calculations which also included the 3^- 9.64 MeV state of ^{12}C assuming it to be $K=0$ and $K=3$. The potential parameters and deformation lengths are listed in Table I. The data set for excitation of the 0^+ 7.65 MeV state in ^{12}C are included for completeness, but no analysis of this state was performed.

calculations. These calculations gave reasonable fits to the 2^+ and 3^- states of ${}^{12}\text{C}$, but the agreement with the elastic scattering and the projectile excitation data was poor. This was to be expected since even the best fits obtained when only states in ${}^7\text{Li}$ were coupled together were not very good.

The mutual excitation data were now included in the calculations. Both the one-step couplings from the elastic scattering to the mutual excitation, and the two-step couplings via the $\frac{1}{2}^-$ state in ${}^7\text{Li}$ and the 2^+ state in ${}^{12}\text{C}$ were included. The elastic scattering was now a little better described, but the angular distributions for the 2^+ and 3^- states of ${}^{12}\text{C}$ were much the same as before, as also was the fit to the $\frac{1}{2}^-$ state of ${}^7\text{Li}$. The prediction for the mutual excitation had little resemblance to the data, just as was found for the DWBA calculations previously.

The calculations were now repeated with coupling terms between the $\frac{1}{2}^-$ state of ${}^7\text{Li}$ and the 2^+ state of ${}^{12}\text{C}$. These couplings have the form of mutual excitation. It was now found necessary to adjust the quadrupole deformation lengths to 1.35 fm for ${}^7\text{Li}$ and -1.05 fm for ${}^{12}\text{C}$ to obtain the correct magnitudes to the projectile and target excitation data. The results of these calculations are shown in Fig. 5 with the parameters given in Table I. The elastic scattering is now reasonably well described except in the region $\theta = 40^\circ - 70^\circ$ where the minima are not deep

enough. The 2^+ state of ${}^{12}\text{C}$ is fairly well fitted. The slope for $\theta < 60^\circ$ is not quite correct, but the large angle magnitude is better than in the target excitation calculations. The description of the 3^- state of ${}^{12}\text{C}$ is much the same as the previous calculations with $K^\pi = 3^-$. The angular distribution for the $\frac{1}{2}^-$ state of ${}^7\text{Li}$ shows some improvements over the projectile excitation calculations. The positions of the forward angle oscillations are correctly placed. The slope is now correct but the minima, as before, are not deep enough. The calculations at large angles now agree well in magnitude with the data. Unfortunately the mutual excitation data are poorly described, there being only qualitative agreement with the calculations. The general magnitude and slope are reasonable, but there is little evidence of the (peculiar) oscillatory nature of the data in the calculations.

There have been very few previous calculations of mutual excitation for ${}^7\text{Li} + {}^{12}\text{C}$. Data are reported at 36 MeV in Ref. 6 but no calculations were made. These data also show a peculiar oscillatory structure similar to that found at 34 MeV here. Zeller *et al.*⁵ measured data at 48 MeV and made some DWBA calculations as referred to above. They did not show the results of their calculations in the figures but the data appear similar to these at the lower energies. Cook *et al.*⁸ have carried out coupled channels calculations for ${}^7\text{Li} + {}^{12}\text{C}$ at 63 and 79 MeV. Reasonably good fits were obtained to the elastic scattering, the $\frac{1}{2}^-$ state of ${}^7\text{Li}$, the 2^+ state of ${}^{12}\text{C}$, and the mutual excitation data. The mutual excitation, which consisted of regularly spaced oscillations, was found to be dominated by the sequential excitation of states in ${}^7\text{Li}$ and ${}^{12}\text{C}$. The calculations at all energies show that the single step direct excitation is important at small angles, where it is dominated by the $l=4$ form factor. The single step contribution decreases rapidly, and at larger angles sequential excitation is required to obtain the correct magnitude. The forward angle data at 63 and 79 MeV are well described by the calculations, whereas the data at 34, 36, and 48 MeV resemble $l=2$ angular distributions more closely than those with $l=4$. We are unable to explain the unusual behavior of the data in the energy region 34–48 MeV and why our calculations are unable to reproduce it.

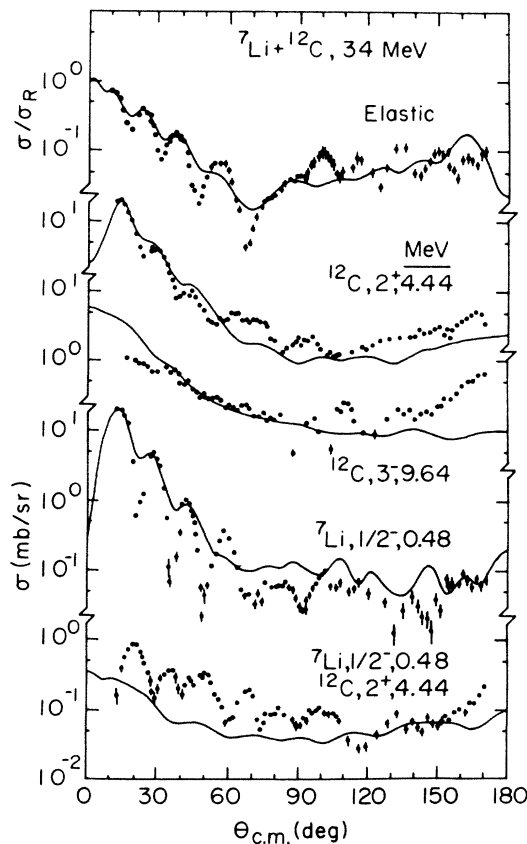


FIG. 5. Results of coupled channels calculations which included projectile, target, and mutual excitation, simultaneously. The potential parameters and deformation lengths are listed in Table I.

IV. SINGLE-NUCLEON TRANSFER DATA

A. Analysis of the (${}^7\text{Li}, {}^6\text{Li}$) reaction

Finite range DWBA calculations were made for the ${}^{12}\text{C}({}^7\text{Li}, {}^6\text{Li}){}^{13}\text{C}$ reaction using the computer program DWUCK5.¹¹ A radius parameter of 1.25 fm, diffuseness of 0.65 fm, and a spin-orbit parameter λ of 25 were used to calculate the bound state wave functions. The depths of the bound state potentials were determined by varying the depths to achieve the correct binding energies. Cohen and Kurath¹² spectroscopic factors for ${}^7\text{Li} \rightarrow {}^6\text{Li} + n$ were used. These have the values $C^2S = 0.431$ for the $1p_{3/2}$ component and $C^2S = 0.289$ for the $1p_{1/2}$ component, and have been shown to be in good agreement with experimental results on many occasions. The entrance channel optical potentials were potentials VII, VIII, and IX for ${}^7\text{Li} + {}^{12}\text{C}$ at 34 MeV from Ref. 4, and for the exit channel

TABLE II. Spectroscopic factors S for ^{13}C .

State	Theory ^a	$(^7\text{Li}, ^6\text{Li})$		(d, p)		(\vec{d}, p)
		34 MeV ^b	48 MeV ^c	2.6–13 MeV ^d	8–26 MeV ^e	
$\frac{1}{2}^-$ 0.0 MeV	0.61	0.65 ± 0.06	0.80	0.58 ± 0.04	0.96 ± 0.25	1.1–1.4
$\frac{1}{2}^+$ 3.09 MeV		0.75 ± 0.08	0.44(0.90)	0.36 ± 0.02	0.9	1.1–1.2
$\frac{5}{2}^+$ 3.85 MeV		0.68 ± 0.10	0.74		0.8	1.1–1.4

^aReference 12.^bThis work.^cReference 5. The value of 0.44 for the $\frac{1}{2}^+$ state is for normalization at forward angles only. The 0.90 result is obtained if all of the data are used to normalize the calculation.^dReference 22.^eReferences 13–17.^fReference 18.

potentials I and II for $^6\text{Li} + ^{12}\text{C}$ at 24 MeV and potentials III and IV for $^6\text{Li} + ^{12}\text{C}$ at 30 MeV from the same reference. All combinations of potentials were tried. The target spectroscopic factors were determined by normalization of the calculations to the experimental data at forward angles.

The experimental data are for population of the $\frac{1}{2}^-$ ground state, the $\frac{1}{2}^+$ 3.09 MeV and $\frac{5}{2}^+$ 3.85 MeV states

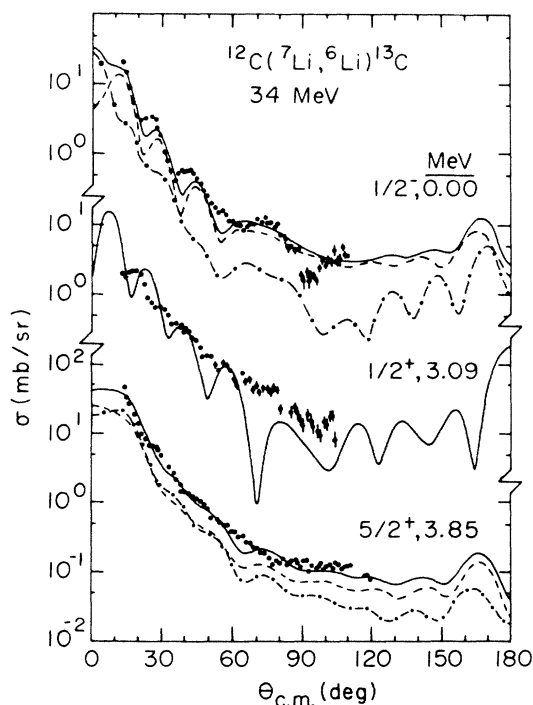


FIG. 6. Finite-range DWBA predictions of the $^{12}\text{C}(^7\text{Li}, ^6\text{Li})^{13}\text{C}$ reaction at 34 MeV compared with experimental data. Contributions coming from the $1p_{3/2}$ and $1p_{1/2}$ components of $^7\text{Li} \rightarrow ^6\text{Li} + n$ are shown separately for the $\frac{1}{2}^-$ ground state and $\frac{5}{2}^+$ 3.85 MeV state of ^{13}C . For the $\frac{1}{2}^+$ 3.09 MeV state they have the same shape, but different magnitudes. The ^7Li and ^6Li optical potentials were obtained from Ref. 4. The calculations shown in the figure used the combinations VIII + III, VIII + III, and VIII + IV for the $\frac{1}{2}^-$, $\frac{1}{2}^+$, and $\frac{5}{2}^+$ states, respectively. The spectroscopic factors for ^{13}C are listed in Table II.

of ^{13}C . These data together with representative “good” fits are shown in Fig. 6. The spectroscopic factors are listed in Table II. The three states were considered as a neutron bound to ^{12}C in $1p_{1/2}$, $2s_{1/2}$, and $1d_{5/2}$ orbitals, respectively.

A spectroscopic factor of 0.65 ± 0.06 was found for the ground state. The $1p_{3/2}$ transfer in $^7\text{Li} \rightarrow ^6\text{Li} + n$ was found to be dominant and the best descriptions of the data were found for the potential combinations VIII + III, IX + II, and IX + III. In particular, calculations with potential VII for ^7Li poorly described the data. This potential has a shallow real part and thus it seems that a deep real potential is preferred in the entrance channel. The calculations describe the shape of the data well but are shifted in phase by about 5° .

There is only an $l=1$ contribution to excitation of the $\frac{1}{2}^+$ 3.09 MeV state in ^{13}C because of selection rules. The $p_{3/2}$ and $p_{1/2}$ transfers for $^7\text{Li} \rightarrow ^6\text{Li} + n$ then give the same angular distributions, apart from the magnitudes. A spectroscopic factor of 0.75 ± 0.08 was found and all the calculations were oscillatory, whereas the data decreases in magnitude smoothly. The potential combinations which fitted the ground state also worked well here, as also did the combinations VII + II and IX + I. Comparing the data and calculations around $\theta=20^\circ$, there is also some evidence for a phase difference of about 5° between them.

A spectroscopic factor of 0.68 ± 0.1 was found for the $\frac{5}{2}^+$ 3.85 MeV state. The $p_{3/2}$ and $p_{1/2}$ transfers for $^7\text{Li} \rightarrow ^6\text{Li} + n$ give approximately equal contributions for $\theta < 60^\circ$, and at larger angles the $p_{3/2}$ component dominates. All the calculations decreased smoothly in the same fashion as the data. The best fits were obtained for potential combinations VII + II, VIII + IV, IX + I, and IX + II.

B. Analysis of the $(^7\text{Li}, ^6\text{He})$ reaction

The same prescription as above was used to make finite range DWBA calculations of the $^{12}\text{C}(^7\text{Li}, ^6\text{He})^{13}\text{N}$ reaction. The Cohen and Kurath¹² spectroscopic factor for $^7\text{Li} \rightarrow ^6\text{He} + p$ is $C^2S=0.592$ for a $1p_{3/2}$ transfer. Calculations were only made for the $\frac{1}{2}^-$ ground state of ^{13}N , assuming the proton to be transferred into a $1p_{1/2}$ orbital. The $\frac{1}{2}^+$ 2.365 MeV state was not observed in the

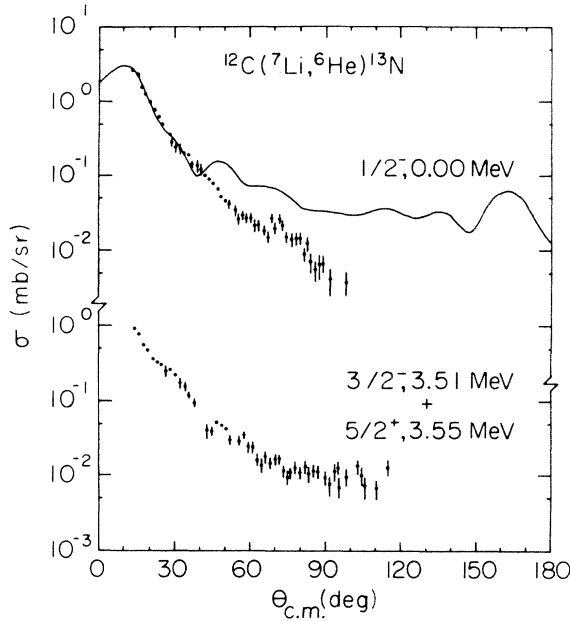


FIG. 7. Experimental data for the ${}^{12}\text{C}({}^7\text{Li}, {}^6\text{He}){}^{13}\text{N}$ reaction at 34 MeV. The results of a finite-range DWBA calculation for the ground state are shown. The ${}^7\text{Li}$ and ${}^6\text{He}$ optical potentials were obtained from Ref. 4. The calculation shown in the figure used the combination VIII + III. The spectroscopic factor for ${}^{13}\text{N}$ is listed in Table III.

$({}^7\text{Li}, {}^6\text{He})$ spectrum. The unbound $\frac{3}{2}^-$ 3.511 MeV and $\frac{5}{2}^+$ 3.547 MeV states were unresolved. At present it is not possible to carry out finite range DWBA calculations to the continuum. There was no great preference for any particular combination of potentials. The experimental data and a fit to the ground state are shown in Fig. 7. A spectroscopic factor $S=0.38\pm 0.05$ was found for the ground state and is compared in Table III with values

TABLE III. Spectroscopic factors S for the ground state of ${}^{13}\text{N}$.

Reaction	E (MeV)	S	Ref.
Theory		0.61	12
$({}^7\text{Li}, {}^6\text{Li})$	34	0.38 ± 0.05	This work
	48	0.72	5
(d,n)	2.6–13	0.53 ± 0.04	22
	11.8	0.74	23
	12–17	0.78–1.35	24
(\vec{d}, n)	5.7–9.7	0.59	25
$({}^3\text{He}, \text{d})$	16–18	0.7–1.48	26
	25.4	0.81	27
$({}^3\vec{\text{He}}, \text{d})$	33	0.68	28

from other reactions. The fit to the data is good for angles less than 40° , being correct in slope and phase, but becomes about three times greater than the data for larger angles.

V. DISCUSSION AND CONCLUSIONS

It is evident from this work that the DWBA is unable to describe the inelastic excitation of the $\frac{1}{2}^-$ 0.478 MeV state in ${}^7\text{Li}$. This state is strongly coupled to the ground state and must be treated in coupled channels calculations, but even then after extensive parameter searching it was not possible to find a Woods-Saxon potential that would fit the projectile excitation data well. A quadrupole deformation length $\delta_2=2.0$ fm was found for ${}^7\text{Li}$ in this study, compared with values in the range 3.5–4.5 fm for the ${}^7\text{Li} + {}^{12}\text{C}$ system at different energies (Table IV). The $B(E2)$ value¹⁹ for ${}^7\text{Li}$ suggests a deformation length of 2.8 fm for the $\frac{3}{2}^- - \frac{1}{2}^-$ transition. There is therefore a discrepancy between these different values. In a paper²⁰

TABLE IV. Deformation lengths for ${}^7\text{Li}$ and ${}^{12}\text{C}$.

Reaction	Type	$\delta_2({}^7\text{Li})$ (fm)	$\delta_2({}^{12}\text{C})$ (fm)	$\delta_{3K}({}^{12}\text{C})$ (fm)
$B(EL)^a$		2.8 ^b	1.48 ^c	
$\text{p} + {}^{12}\text{C}$	30–40 MeV ^d	CC, RVM	–1.62	1.11 $K=0$ 0.86 $K=3$
${}^6\text{Li} + {}^{12}\text{C}$	24 MeV ^e	CC, RVM	–1.25	0.90 $K=0$ 0.40 $K=3$
	30 MeV ^e	CC, RVM	–1.25	0.90 $K=0$ 0.25 $K=3$
${}^7\text{Li} + {}^{12}\text{C}$	34 MeV ^f	CC, RVM	–1.40	1.11 $K=0$ 0.82 $K=3$
	36 MeV ^g	DWBA	3.5	1.52
	48 MeV ^h	DWBA	4.17/4.50	1.4/1.52
	63 MeV ⁱ	DWBA	3.77/4.18	1.47/1.44
	79 MeV ⁱ	DWBA	3.61/4.22/3.96	1.28/1.44/1.41

^aDeformation lengths calculated from $B(EL)$ values.

^bReference 19.

^cReference 21.

^dReference 10.

^eReference 9.

^fPresent work.

^gReference 6.

^hReference 5.

ⁱReference 7.

on projectile excitation for ${}^7\text{Li} + {}^{40}\text{Ca}$ at 34 MeV a deformation length for ${}^7\text{Li}$ of 1.95 fm was found if Woods-Saxon potentials were used, and 3.28 fm for folded potentials and form factors. These results suggest that the influence of the interaction potential on the derived deformation parameters is poorly understood for a highly deformed projectile like ${}^7\text{Li}$.

The 2^+ 4.44 MeV state in ${}^{12}\text{C}$ is strongly coupled to the ground state and is not well described by the DWBA. With coupled channels calculations good fits were obtained to the elastic data and it was possible to fit the data for the 2^+ state forward of 50° but the magnitude was too small at larger angles. A quadrupole deformation length of -1.40 fm for ${}^{12}\text{C}$ was found in this study. From the phasing of the calculations compared with the data the sign was unambiguously determined to be negative. This compares well (Table IV) with values in the range ± 1.3 – 1.5 fm from DWBA calculations for ${}^7\text{Li} + {}^{12}\text{C}$ at higher energies, and with ± 1.48 fm from the $B(E2)$ value. It is a little smaller in magnitude than the value of -1.62 fm found from $p + {}^{12}\text{C}$, and a little more than the ${}^6\text{Li} + {}^{12}\text{C}$ value of -1.25 fm. The quadrupole deformation length obtained here therefore seems compatible with those determined previously.

The 3^- 9.64 MeV state is weakly coupled and can be described well by DWBA calculations which fail to distinguish between $K=0$ and $K=3$ for this state in the rotation vibration model. When coupled channels calculations using the rotation vibration model are carried out, there is a definite preference for $K=3$ for the 3^- state. In the three-alpha cluster model of ${}^{12}\text{C}$ this corresponds to a triangular configuration of the three-alpha clusters. We note that a previous study⁹ of ${}^6\text{Li} + {}^{12}\text{C}$ inelastic scattering using the rotation-vibration model was unable to determine whether $K=0$ or 3, but for $p + {}^{12}\text{C}$ (Ref. 10) there was an unambiguous assignment of $K=3$. For the octupole deformation length we have only made comparisons with previous studies that used the rotation-vibration model: $p + {}^{12}\text{C}$ (Ref. 10) and ${}^6\text{Li} + {}^{12}\text{C}$.⁹ The values obtained here of 1.11 and 0.82 fm for $K=0$ and $K=3$ are almost identical to those found for $p + {}^{12}\text{C}$, whereas the ${}^6\text{Li} + {}^{12}\text{C}$ values are substantially smaller and also show some energy dependence.

Both the DWBA and CC calculations we have made are unable to fit the data for the mutual excitation of ${}^7\text{Li}$ to its $\frac{1}{2}^-$ 0.478 MeV state and ${}^{12}\text{C}$ to its 2^+ 4.44 MeV state. This may be related to the problem of describing the projectile excitation data by itself.

In the present case, the breakup cross sections are dominated by the direct process. The direct breakup cross section is about 25 times larger than the sequential cross sec-

tion through the 4.63 MeV state in ${}^7\text{Li}$. At a ${}^7\text{Li}$ energy of 70 MeV, it has been reported²⁹ that the ${}^7\text{Li}$ breakup process is predominantly sequential, proceeding through the 4.63 MeV state of ${}^7\text{Li}$. The energy dependence of the observed breakup process is opposite to that expected. As the bombarding energy increases the direct breakup mode should become dominant. The two measurements on ${}^{12}\text{C}$ taken to date show that further studies of the energy dependence of the breakup process are needed before a reasonable picture of this process can be obtained at intermediate energies.

Finite-range DWBA calculations were made for the ${}^{12}\text{C}({}^7\text{Li}, {}^6\text{Li}){}^{13}\text{C}$ reaction. For the ground state the calculations describe the data reasonably, except for a phase difference between the two. The calculations for the $\frac{1}{2}^+$ 3.09 MeV state in ${}^{13}\text{C}$ are too oscillatory, but fit the data very well for the $\frac{5}{2}^+$ 3.85 MeV state. The intermediate-coupling model¹² predicts a spectroscopic factor of 0.61 for the ground state compared with 0.65 ± 0.06 from the present work. Table III shows that other (${}^7\text{Li}, {}^6\text{Li}$) and (d,p) calculations have obtained values ranging from 0.80 to 1.40 for this state. The relative spectroscopic factors for the three states are in reasonable agreement for the different studies if the value of 0.9 is used for the $\frac{1}{2}^+$ state for (${}^7\text{Li}, {}^6\text{Li}$) at 48 MeV.

The ${}^{12}\text{C}({}^7\text{Li}, {}^6\text{He}){}^{13}\text{N}$ reaction to the ground state of ${}^{13}\text{N}$ was well described at forward angles by finite-range DWBA calculations. A spectroscopic factor of 0.38 ± 0.05 is obtained from the present work compared with 0.61 from the intermediate-coupling model.¹² Values of 0.53 to 1.48 have been found from previous (${}^7\text{Li}, {}^6\text{He}$), (d,n), and (${}^3\text{He}, \text{d}$) calculations (Table III). Theoretically the ground states of ${}^{13}\text{C}$ and ${}^{13}\text{N}$ should have the same spectroscopic factors since they are mirror nuclei. The shell model calculations of Cohen and Kurath¹² predict $S=0.61$ for both nuclei. Experimentally Pearson *et al.*²² find $S=0.58$ for ${}^{13}\text{C}$ and $S=0.53$ for ${}^{13}\text{N}$ using the (d,p) and (d,n) reactions, while Zeller *et al.*⁵ find $S=0.80$ for ${}^{13}\text{C}$ and $S=0.72$ for ${}^{13}\text{N}$ using the (${}^7\text{Li}, {}^6\text{Li}$) and (${}^7\text{Li}, {}^6\text{He}$) reactions. Thus the equality of these spectroscopic factors is confirmed by experiment. The spectroscopic factor for ${}^{13}\text{N}$ from this study would therefore appear to be unusually low.

ACKNOWLEDGMENTS

The work carried out at Florida State University was funded in part by the National Science Foundation and the State of Florida. Two of us (J.C. and A.K.A.) gratefully acknowledge the support of the University of Petroleum and Minerals.

¹A. C. L. Bernard, J. B. Swint, and T. B. Clegg, Nucl. Phys. 86, 130 (1966).

²H. G. Bingham, A. R. Zander, K. W. Kemper, and N. R. Fletcher, Nucl. Phys. A173, 265 (1971).

³P. D. Kunz (unpublished); modifications by J. R. Comfort, 1979; J. Cook, 1984.

⁴M. F. Vineyard, J. Cook, K. W. Kemper, and M. N. Stephens,

Phys. Rev. C 30, 916 (1984).

⁵A. F. Zeller, K. W. Kemper, D. C. Weissner, T. R. Ophel, D. F. Hebbard, and A. Johnston, Nucl. Phys. A323, 477 (1979).

⁶P. Schumacher, N. Ueta, H. H. Duhm, K.-I. Kubo, and W. J. Klages, Nucl. Phys. A212, 573 (1973).

⁷A. F. Zeller, Y.-W. Lui, R. E. Tribble, and D. M. Tanner, Phys. Rev. C 22, 1534 (1980).

- ⁸J. Cook, N. M. Clarke, J. Coopersmith, and R. J. Griffiths, Nucl. Phys. **A386**, 346 (1982).
- ⁹J. Cook, Nucl. Phys. **A445**, 350 (1985).
- ¹⁰R. De Leo, G. D'Erasmus, A. Pantaleo, M. N. Harakeh, E. Cereda, S. Micheletti, and M. Pignanelli, Phys. Rev. C **28**, 1443 (1983).
- ¹¹P. D. Kunz (unpublished).
- ¹²S. Cohen and D. Kurath, Nucl. Phys. **73**, 1 (101); **A101**, 1 (1967).
- ¹³J. E. Poling, E. Norbeck, and R. R. Carlson, Phys. Rev. C **13**, 648 (1976).
- ¹⁴E. W. Hamburger, Phys. Rev. **123**, 619 (1961).
- ¹⁵J. P. Schiffer, G. C. Morrison, R. H. Siemssen, and B. Zeidman, Phys. Rev. **164**, 1274 (1967).
- ¹⁶R. J. Slobodrian, Phys. Rev. **126**, 1059 (1962).
- ¹⁷R. N. Glover and A. D. W. Jones, Nucl. Phys. **84**, 673 (1966).
- ¹⁸S. E. Darden, S. Sen, H. R. Hiddleston, J. A. Aymar, and W. A. Yoh, Nucl. Phys. **A208**, 77 (1973).
- ¹⁹G. J. C. van Niftrik, L. Lapikas, H. deVries, and G. Box, Nucl. Phys. **A174**, 173 (1971); W. J. Vermeer, M. T. Esat, M. P. Fewell, R. H. Spear, A. M. Baxter, and S. M. Burnett, Phys. Lett. **138B**, 365 (1984).
- ²⁰D. P. Sanderson, S. P. Van Verst, J. Cook, K. W. Kemper, and J. S. Eck, Phys. Rev. C **32**, 887 (1985).
- ²¹F. Ajzenberg-Selove, Nucl. Phys. **A248**, 1 (1976).
- ²²C. S. Pearson, J. M. Covan, D. Zissermann, T. G. Miller, F. P. Gibson, R. Haglund, W. Morrison, and G. Wesley, Nucl. Phys. **A191**, 1 (1972).
- ²³G. S. Mutchler, D. Rendic, D. E. Velkley, W. E. Sweeney, Jr., and G. C. Phillips, Nucl. Phys. **A172**, 469 (1971).
- ²⁴S. Gangardharan and R. L. Wolke, Phys. Rev. C **1**, 1333 (1970).
- ²⁵R. K. Tenhahen and P. A. Quin, Nucl. Phys. **A271**, 173 (1976).
- ²⁶H. T. Fortune, T. J. Gray, W. Trost, and N. R. Fletcher, Phys. Rev. **179**, 1033 (1969).
- ²⁷R. R. Sercely, R. J. Peterson, P. A. Smith, and E. R. Flynn, Nucl. Phys. **A324**, 53 (1979).
- ²⁸O. Karban, S. K. Basak, J. B. A. England, G. C. Morrison, J. M. Nelson, S. Roman, and G. G. Shute, Nucl. Phys. **A269**, 312 (1976).
- ²⁹A. C. Shotter, A. N. Bice, J. M. Wouters, W. D. Rae, and J. Cerny, Phys. Rev. Lett. **46**, 12 (1981).